

Influence of Emitted Electrons on the Method for Direct Measurement of Condensate Resistance

T. Jukna¹, V. Sinkevicius¹, L. Urbanaviciute^{1,2}

¹Department of Electrical Engineering, Kaunas University of Technology,
Daukanto St. 12–103, LT-35212 Panevezys, Lithuania

²Department of Electrical and Electronics Engineering, Panevezys College,
Laisves Sq. 23–117, LT-35200 Panevezys, Lithuania
vytenis.sinkevicius@ktu.lt

Abstract—Electrical resistance of the vacuum-deposited condensate has non-linear relation to the condensate film thickness. Therefore, there exists a need for experiments to study applicability of the non-invasive method for condensate resistance measurement and to identify parameters by measuring condensate resistance directly. By using two-point measurement probes, this study analyses the influence of electrons emitted in the process of evaporator electronic emission on the method for direct measurement of condensate resistance.

Index Terms—Thin film devices, vacuum technology, electrical resistance measurement.

I. INTRODUCTION

Mathematical models [1], [2] of non-invasive methods for measurement of vacuum-deposited condensates describe quite precisely the measurement method itself. This measurement method utilises a flow of electrons emitted from the hot evaporator. The electron flow highly depends on the evaporator temperature, its design, and spatial configuration of grounded metal elements in a vacuum chamber. Magnetic fields in a vacuum chamber and also their direction and strength have a significant impact on the non-invasive measurement method. Main source of magnetic field in a chamber is heating current, which flows in the evaporator as in a closed circuit and usually reaches from 50 A to 300 A. If the evaporator is heated by alternating current, generally there are no stable electron flows in a vacuum evaporation chamber, and their strength and direction fluctuate periodically. Experiments utilizing alternating current controlled by the thyristor converter allowed finding just a short time period, during which probes measured stable electric charge flows [3]. Therefore, further experiments utilized DC stabilized voltage for evaporator heating. This allowed getting stable electric charge flows over the time span.

The other disadvantage of the non-invasive method for resistance measurement is the fact that electrical resistance of the growing condensate film has non-linear relation to the

condensate film thickness [4]. Therefore, there exists a need for experiments to study applicability of the non-invasive method for condensate resistance measurement and to identify parameters by measuring condensate resistance directly. This can be implemented using conventional two- or four-point [5] measurement probes, on which metal condensation takes place. During the process of evaporation, both the hot evaporator and material being evaporated emit electrons, the flow of which reaches the condensation surface. This particular electron flow is used in the non-invasive method for condensate resistance measurement [2]. However, electrons above the surface of two- or four-point measurement probes can also influence the accuracy of the direct condensate resistance measurement [6].

By using two-point measurement probes, this study analyses the influence of electrons emitted in the process of evaporator electronic emission on the method for direct measurement of condensate resistance.

II. MATHEMATICAL MODEL OF CONDENSATE RESISTANCE MEASUREMENT USING DC STABILIZER

Earlier developed mathematical model for measurement of depositing condensate resistance [1] was complemented. This model additionally includes stabilized probe current i_s (Fig. 2).

Condensate resistance measurement probe (Fig. 1) consists of insulating material substrate 1 with width b having metallized areas 2 and 3.

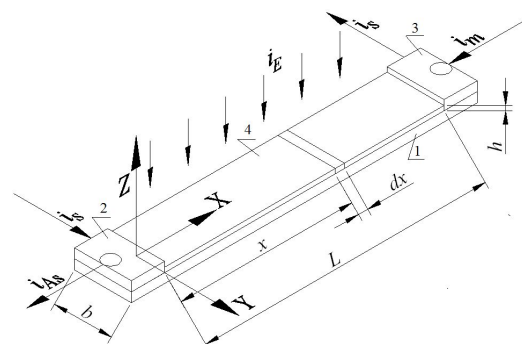


Fig. 1. Condensate resistance measurement probe: 1 – insulating material substrate, 2 – contact area A, 3 – contact area B, 4 – condensate film.

Distance between areas equals to L . Molecules of the material being evaporated hit the probe plane XY in the direction of Z-axis. Ionized atoms and electrons emitted in the process of thermoelectronic emission reach this area too. As the distance between the probe plane XY and the evaporator is long, density of electric charge and material atom flow forming the condensate 4 between contact areas 2 and 3 is uniform.

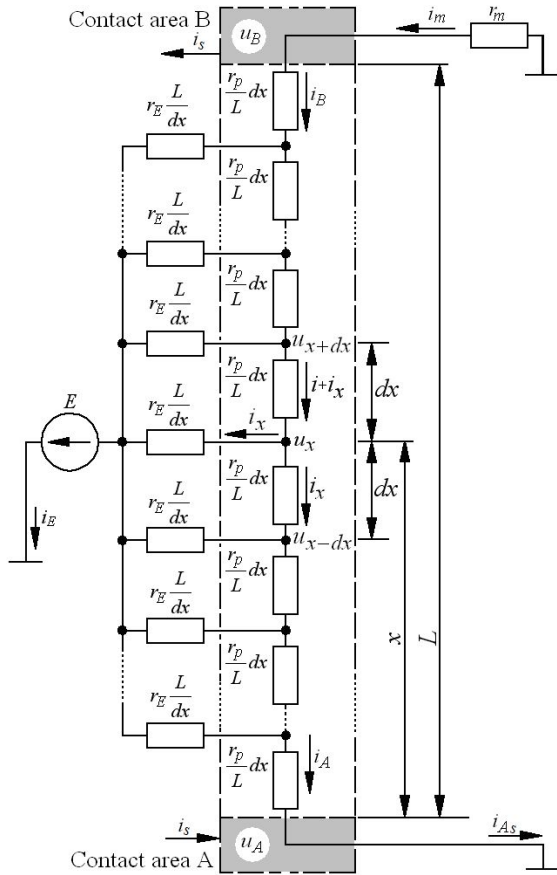


Fig. 2. Schematic circuit diagram of the condensate resistance measurement model, where contact area A is grounded, and contact area B is connected to the ground through the resistance r_m . Additionally, stabilized current i_s flows through the probe.

Mathematical model [1] assumes that condensate 4 formation rate in between contact areas A and B is uniform (Fig. 1); condensate resistance denoted as r_p . As during early formation stages condensate is deposited in islands, value h denotes the equivalent condensate thickness. For model development purposes, condensate strip 4 is divided into sub-strips with length dx (Fig. 2), width b , and thickness h . The equivalent resistance of the electric charge flow i_E denoted as r_E . To simplify the model, r_E assumed as constant.

As the evaporator is powered from a direct current source, electron flow of the thermoelectronic emission is exposed to constant electromagnetic and electrostatic fields. These fields change the direction of the electron flow away from the substrate aligned perpendicularly to the evaporator. This results in reduced measurements of the voltage on measurement probes. As a consequence, this method is only applicable for analysis of materials with very high evaporation temperatures. However, the solution was found to expand method application limits.

It utilizes additional electron source (tungsten filament) placed closer to measurement probes by $2/3$ of the total distance to the evaporator. This distance selected to ensure the minimum influence of the electromagnetic field on the electron source and, at the same time, for it not to be too close to the probes to prevent temperature of the film being formed from rising above the allowable limit. The solution enabled measuring resistance of films condensed from conductive materials with low evaporation temperatures. It also contributed to stabilizing values of the thermal EMF source and r_E without any noticeable impact on the film growth. During the model development, thermoelectromotive force E of this additional electron source has been also included.

Potential u_x of the sub-strip with width dx relates to the distance x till the area A as follows

$$\frac{d^2 u_x}{dx^2} - \frac{r_p}{r_E L^2} u_x = -\frac{r_p}{r_E L^2} E. \quad (1)$$

Characteristic roots of the differential equation (1) are as follows

$$\lambda_{1,2} = \pm \frac{1}{L} \sqrt{\frac{r_p}{r_E}} = \pm \frac{1}{L}. \quad (2)$$

Common solution of (1) is as follows

$$u_x = C_1 e^{\frac{x}{L}} + C_2 e^{-\frac{x}{L}} + E. \quad (3)$$

Expression of the current i_x in the substrate has also been obtained

$$i_x = \frac{S}{r_p} \left(C_1 e^{\frac{S}{L} x} - C_2 e^{-\frac{S}{L} x} \right). \quad (4)$$

Coefficients C_1 and C_2 depend on the initial conditions on contact areas A and B, i.e. on the probe connection in the measurement circuit. This study analyses circuit diagram where the probe area A is grounded and the measurement takes place of the area B potential u_B , which is caused by the voltage drop on the resistance r_m (Fig. 3). As the area A is grounded, initial conditions obtained from (3) are as follows

$$0 = C_1 + C_2 + E. \quad (5)$$

In case of stabilized current i_s , we can write for the node of the area B as follows: $i_m - i_B - i_s = 0$. Then, the potential of the area B is calculated as follows

$$u_B = i_s r_m - \frac{S r_m}{r_p} \left(C_1 e^{S} - C_2 e^{-S} \right). \quad (6)$$

By inserting (6) into (3) and by factoring common members the following is obtained

$$-E + i_s r_m = C_1 e^S \left(1 - S r_m / r_p \right) +$$

$$+C_2 e^{-S} (1 + S r_m / r_p). \quad (7)$$

To find coefficients C_1 and C_2 from (5) and (7), system of equations is made:

$$\begin{cases} C_1 e^S (1 + A) + C_2 e^{-S} (1 - A) = -E + i_s r_m, \\ C_1 + C_2 = -E, \end{cases} \quad (8)$$

where $A = -\frac{r_m}{r_p}$.

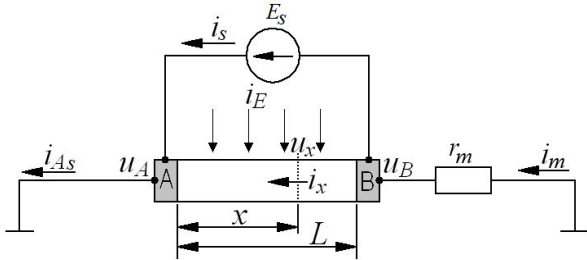


Fig. 3. Connection diagram of the condensate resistance measurement probe.

Considering expressions of C_1 , C_2 [1], relation of condensate potential u_x to the distance x is expressed as follows

$$u_x = \frac{-E}{D} \left[e^{x \frac{S}{L}} - e^{-x \frac{S}{L}} e^{\frac{xS}{L}} (1 - A) - e^{-x \frac{S}{L}} + e^S e^{-x \frac{S}{L}} (1 + A) \right] + E + \frac{i_s r_m}{D} \left(e^{x \frac{S}{L}} - e^{-x \frac{S}{L}} \right), \quad (9)$$

where $D = e^S - e^{-S} + A(e^S + e^{-S})$.

By replacing the distance x in (9) with the distance L between areas A and B, relation of the contact area B potential u_B to and, at the same time, to the resistance r_p is obtained

$$u_B = \frac{(e^S - e^{-S})(-E + i_s r_m) - 2EA}{e^S - e^{-S} + A(e^S + e^{-S})} + E. \quad (10)$$

For the model development purposes, it is assumed that condensate formation rate is constant, i.e. condensate thickness has linear relation to time: $h = f(t)$. Due to this reason, modelling results are presented as a relation to the substrate resistance r_p , which is inversely proportional to the thickness: $r_p = 1/h(t)$.

Figure 4 shows how the trend of potential u_B (10) relates to the condensate resistance r_p according to EMF changes in the additional thermoelectric emission source.

The results presented show (Fig. 4) that additional thermoelectric emission source contributes to higher values of the voltage u_B . Changes of the EMF in the additional thermoelectric emission source cause shifts of the voltage u_B extremum. Reduction of this EMF results in

shifting the extremum of u_B towards the range of higher substrate resistances r_p .

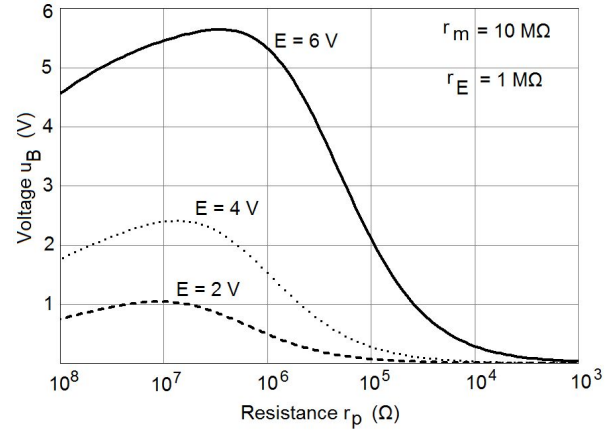


Fig. 4. Relation of the potential u_B to the condensate resistance r_p according to different values of the emf in the additional thermoelectric emission source. Stabilized current $i_s = 0$.

Figure 5 presents voltage u_B (10) modelling results obtained using stabilized current source with maximum voltage of 8 V and setting stabilized substrate current $i_s = 2 \mu\text{A}$. Modelling performed with additional thermoelectric emission source voltage of 6 V and measuring device resistance $r_m = 10 \text{ M}$.

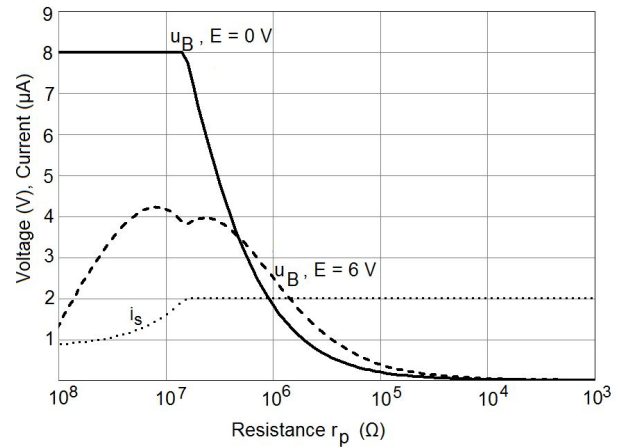


Fig. 5. Relation of the potential u_B to the condensate resistance r_p . Stabilized current $i_s = 2 \mu\text{A}$.

Results in Fig. 5 show that measurement of the substrate resistance r_p without additional thermoelectric emission source (corresponds to the state of closed shutter) can only be started after the current stabilizer changes its status from saturation and starts stabilizing the current. With the fixed value of stabilized current $i_s = 2 \mu\text{A}$ and with the shutter open (thermoelectric emission source voltage of 6 V), the substrate voltage u_B relates to the stabilized current value. Modelling results allow concluding that additional thermoelectric emission source will impact on measurement results; therefore, galvanic isolation of resistance measurement and additional thermoelectric emission source circuits is necessary.

To check the modelling results, growing condensate resistance was measured using both direct and non-invasive methods. Modelling results also allow concluding that direct measurement of the substrate resistance will only be possible when the current stabilizer changes its status from saturation.

III. DIRECT METHOD OF CONDENSATE RESISTANCE MEASUREMENT

Circuit diagram of the experiment is presented in Fig. 6. Experiment utilizes three identical substrates P1, P2, and P3 located one beside the other.

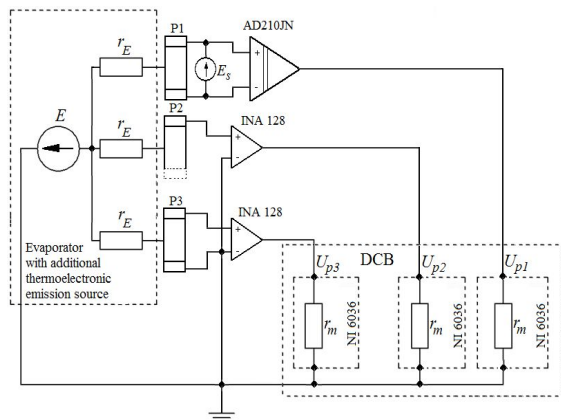


Fig. 6. Experimental circuit diagram for growing condensate measurement.

After setting evaporation parameters (evaporator powered from 15 V adjustable power source), the shutter is opened and vapour flow reaches substrates. Resistance of the substrate P1 is measured directly, using two-point measurement probes. Contact areas of the substrate P1 connected to the stabilized current source (Fig. 6) which, for the purpose of experiments, had its voltage set to 8 V and provided substrate current $i_s = 2 \mu\text{A}$. In the process of the experiment, voltage drop U_{p1} on the substrate P1 film was measured during the course of its formation. As we can see from the above modelling results, this measurement method requires galvanic isolation of the substrate P1 from the common system ground; otherwise, electron flow from the additional thermoelectronic emission source (additional electron source is powered by the voltage of 6 V) impacts on measurements results, and this prevents from determining the substrate resistance correctly. AD210JN galvanically isolated operational amplifier used for this purpose. This amplifier also contributed in reducing noise impact due to long measurement leads.

Substrates P2 and P3 were intended for their resistance measurement using electron emission current. The substrate P3 has two contact areas; one of them is connected to the system's ground and the other to the data collection board (DCB) through INA128 operational amplifier installed within the vacuum chamber beside the substrate. The operational amplifier reduces noise impact due to connecting leads. Contact area of the substrate P2 is also connected to DCB through the operational amplifier. The substrate P2 has no second contact area. In the process of the experiment, substrate voltages U_{p2} and U_{p3} were measured respectively. Results of the experiment are presented in Fig. 7.

As we can see, resistance measurement by the direct method can only be performed at a certain time period. This section within which the measurement is possible denoted as H in Fig. 7. Substrate resistance can be calculated as follows

$$r_p = \frac{U_{p1}}{i_s}. \quad (11)$$

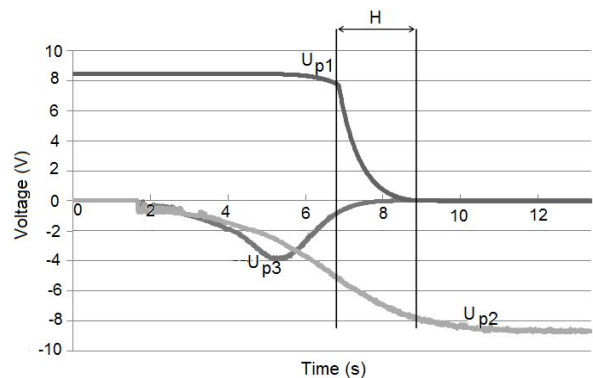


Fig. 7. Voltage drop on each of the substrates during the course of film formation.

For comparison purposes, Fig. 7 also shows voltages U_{p2} and U_{p3} of non-invasive measurement probes with one and two contacts. As we can see, the signal measured by the non-invasive method starts changing from the beginning of condensation, i.e. much earlier before reaching interval H .

IV. CONCLUSIONS

By properly selecting design of emission source and value of stabilized current, direct condensate resistance measurement is possible within the section of substrate voltage decrease. In case on non-invasive measurement method which utilizes probe with two contacts (Fig. 7), trend contains pronounced extremum that can be useful in control for getting desired layer thickness of the material being evaporated. It was proven that electron flow from the thermoelectronic emission source has an impact on direct resistance measurement signal, and therefore, it is necessary to galvanically isolate circuits of resistance measurement and additional thermoelectronic emission source.

REFERENCES

- [1] V. Sinkevicius, "The mathematical model of conductance measurement in growing thin films", *Elektronika ir elektrotechnika (Electronics and Electrical Engineering)*, no. 5, pp. 17–20, 2008.
- [2] V. Sinkevicius, "Research of the method opportunities of growing films conductance measurement", *Elektronika ir elektrotechnika (Electronics and Electrical Engineering)*, no. 4, pp. 71–74, 2009.
- [3] V. Sinkevicius, D. Virzonis, L. Sumskiene, T. Jukna, "Research of electrodynamic processes in vacuum evaporation system", *Elektronika ir elektrotechnika (Electronics and Electrical Engineering)*, no. 4, pp. 75–78, 2007.
- [4] H. D. Liu, Y. P. Zhao, G. Ramanath, S. P. Murarka, G. C. Wang, "Thickness dependent electrical resistivity of ultrathin (<40 nm) Cu films", *Thin Solid Films*, vol. 384, pp. 151–156, 2001. [Online]. Available: [http://dx.doi.org/10.1016/S0040-6090\(00\)01818-6](http://dx.doi.org/10.1016/S0040-6090(00)01818-6)
- [5] Sh. Yoshimoto, Y. Murata, K. Kubo, K. Tomita, K. Motoyoshi, T. Kimura, H. Okino, R. Hobara, I. Matsuda, Sh. Honda, M. Katayama, Sh. Hasegawa, "Four-point probe resistance measurements using PtIr-coated carbon nanotube tips", *Nano Lett.*, vol. 7, no. 4, pp. 956–959, 2007. [Online]. Available: <http://dx.doi.org/10.1021/nl0630182>
- [6] M. Novotny, J. Bulir, J. Lancok, P. Pokorný, M. Bodnar, "In-situ monitoring of the growth of nanostructured aluminium thin film", *Journal of Nanophotonics*, vol. 5, no. 1, pp. 1–10, 2011.